S. Figure 1

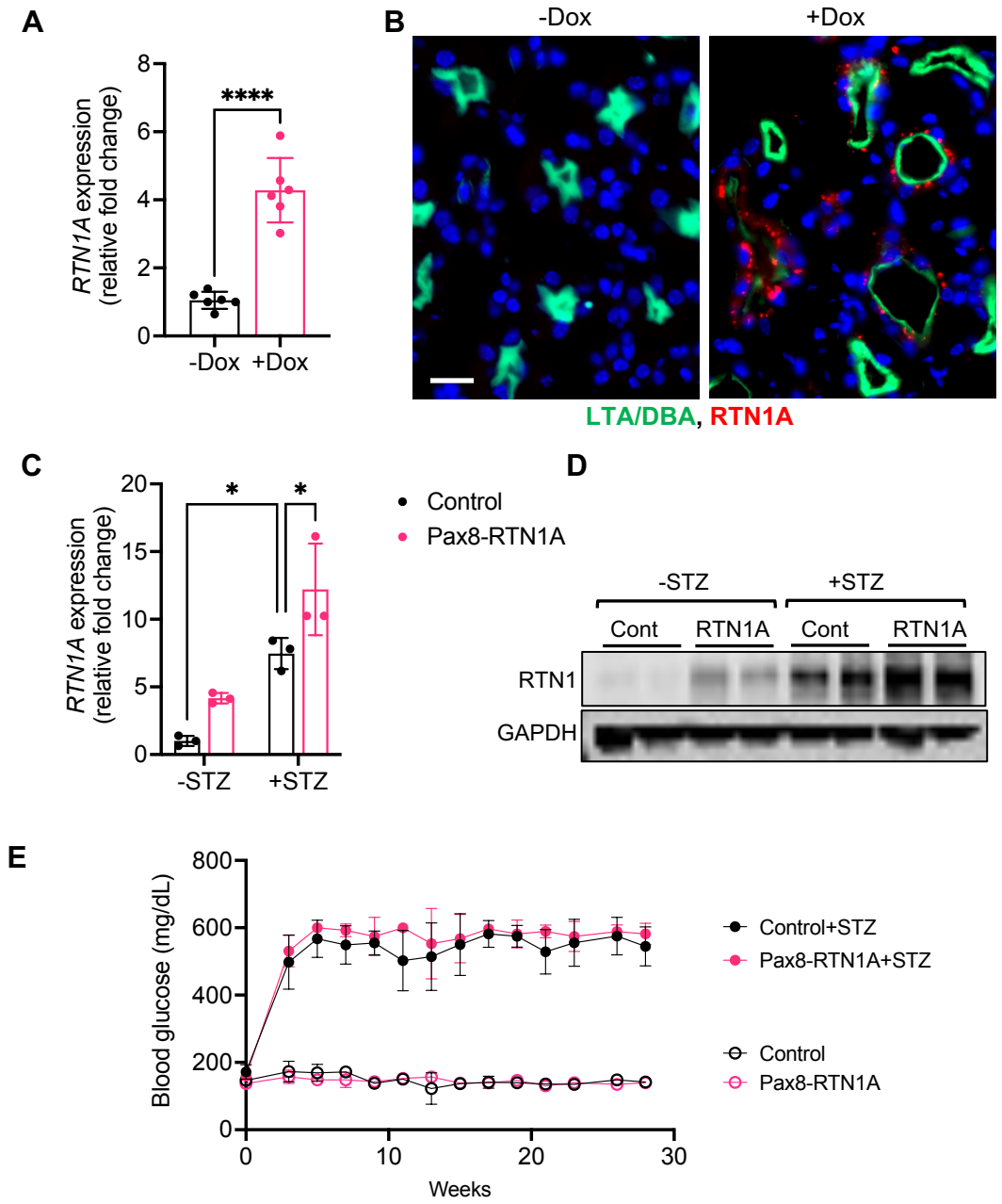

Supp. Fig. 1: Induction of RTN1A overexpression in control and diabetic mice. (A-B) RTN1A was induced in 8-week old Pax8-rtTA;TRE-RTN1A mice with doxycycline (Dox)-supplemented (625mg/kg) chow for three weeks. Real-time PCR analysis of *RTN1A* mRNA using a primer pair that simultaneously detects mouse and human transcripts is shown as a relative fold change to no Dox control (n=6 mice per group). ****P<0.0001 by unpaired, two-tailed t-test. (B) Immunostaining of RTN1A (red) on frozen kidney tissues. Lotus tetragonolobus agglutinin (LTA) and Dolichos biflorus (DBA) lectins (green) were also used to detect proximal and distal collecting duct cells. Scle bar, 20µm. (C) Real-time PCR analysis of RTN1A expression in diabetic (+STZ) and non-diabetic (-STZ) mice. *P<0.05 between indicated groups by 2-way ANOVA with Tukey's post hoc test. (D) Western blot analysis of RTN1A in kidney cortex of mice (n=2 mouse samples per group). Anti-RTN1A antibody (MON162) detects both murine and human RTN1A. (E) Blood glucose levels of diabetic and non-diabetic mice after STZ or vehicle injection [*n.b.* as maximum reading on the glucometer is 600mg/dL, the actual numbers in diabetic mice may be higher than indicated on the graph].

S. Figure 2

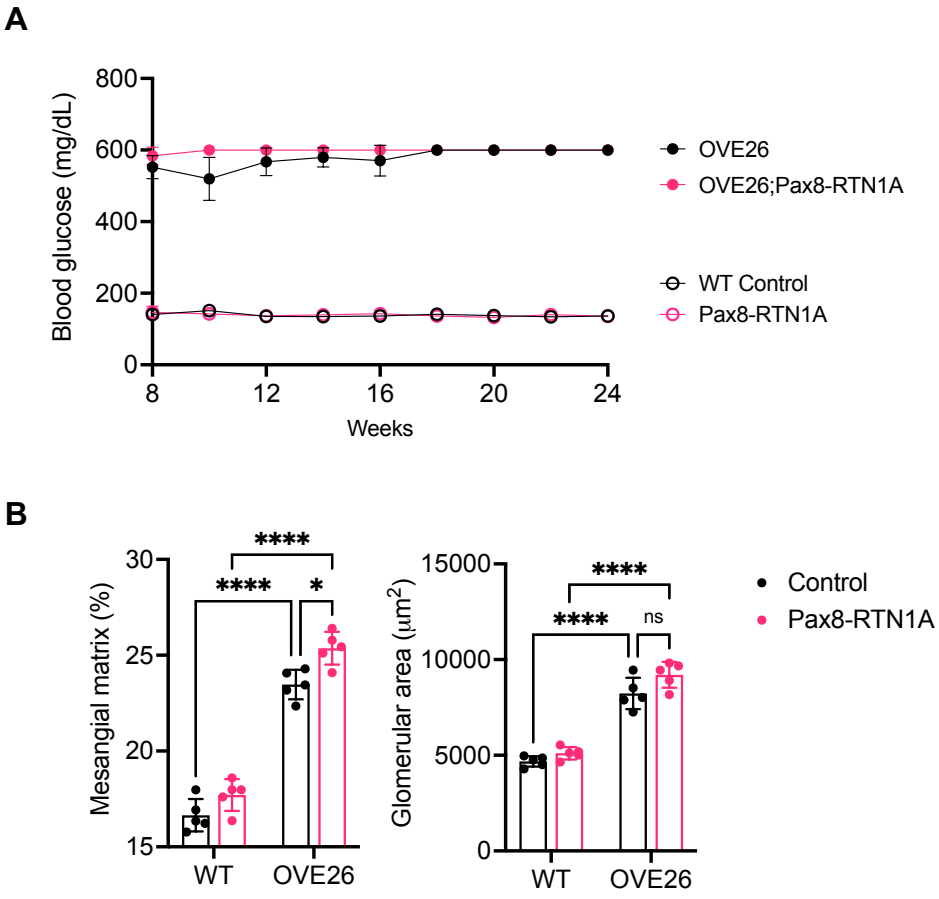

Supp. Fig. 2: RTEC-specific RTN1A overexpression in wildtype (WT) and OVE26 diabetic mice. (A) Average blood glucose measurements of WT and OVE26 mice from 8 to 24 weeks of age [*n.b.* as the maximum reading on the glucometer is 600mg/dL, the actual numbers in diabetic mice are llikely to be higher than indicated on the graph and results in diminished standard deviation]. (B) Quantification of average mesangial matrix fraction (%) and glomerular area is shown per mouse (n=5 mice per group, 20-30 glomeruli evaluated per mouse).*p<0.05 and ****p<0.0001 between indicated groups by two-way ANOVA with Tukey's post hoc analysis.

S. Figure 3

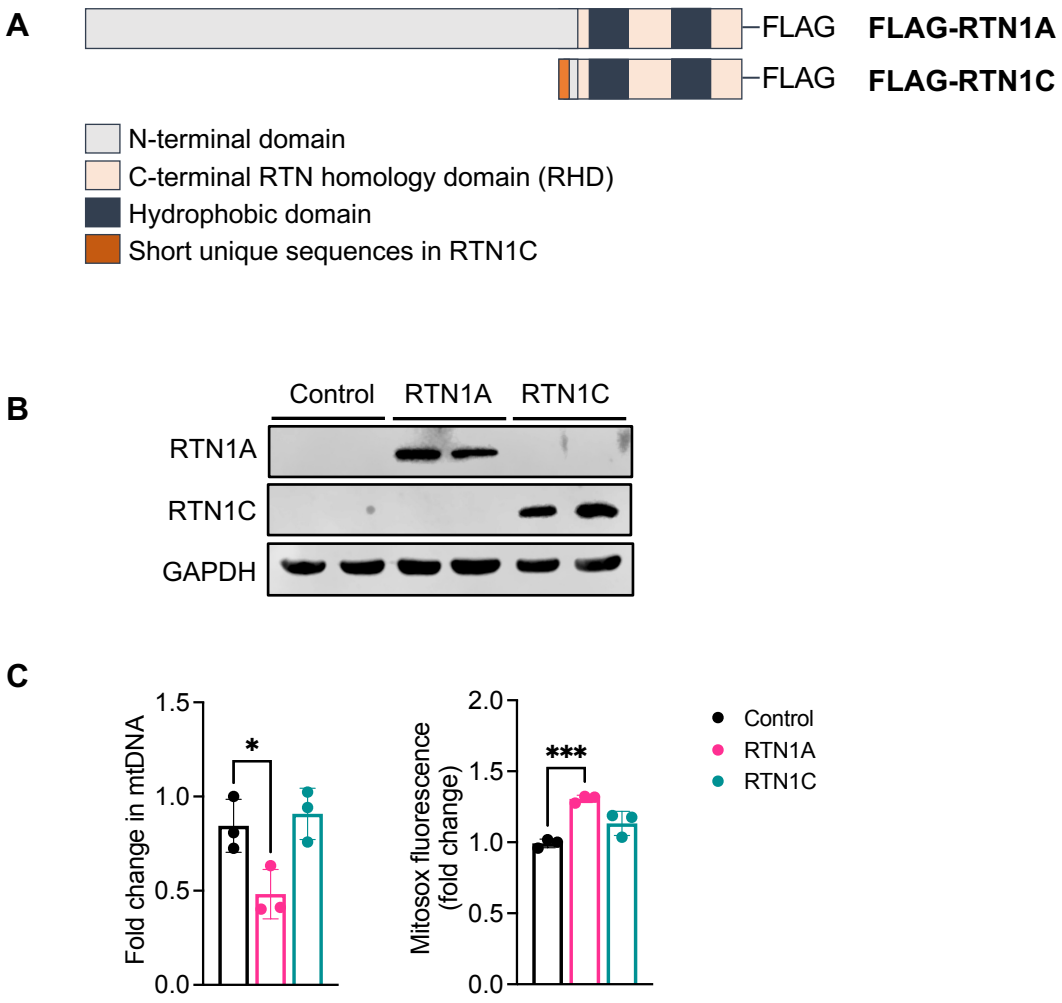

Supp. Fig. 3: RTN1A overexpression, but not RTN1C overexpression, in HK-2 cells leads to altered mitochondrial function. (A) Schematic representation of FLAG-tagged RTN1A and RTN1C proteins. (B) Anti-FLAG western blot analysis of lysates of HK2 cells with overexpression of either FLAG-tagged RTN1A or RTN1C is shown. (C) Average fold change in mtDNA and Mitosox fluorescence in control of RTN1A or RTN1C expressing HK2 cells. *p<0.05 and ***p<0.001 between indicated groups by one-way ANOVA with Tukey's post hoc analysis.

S. Figure 4

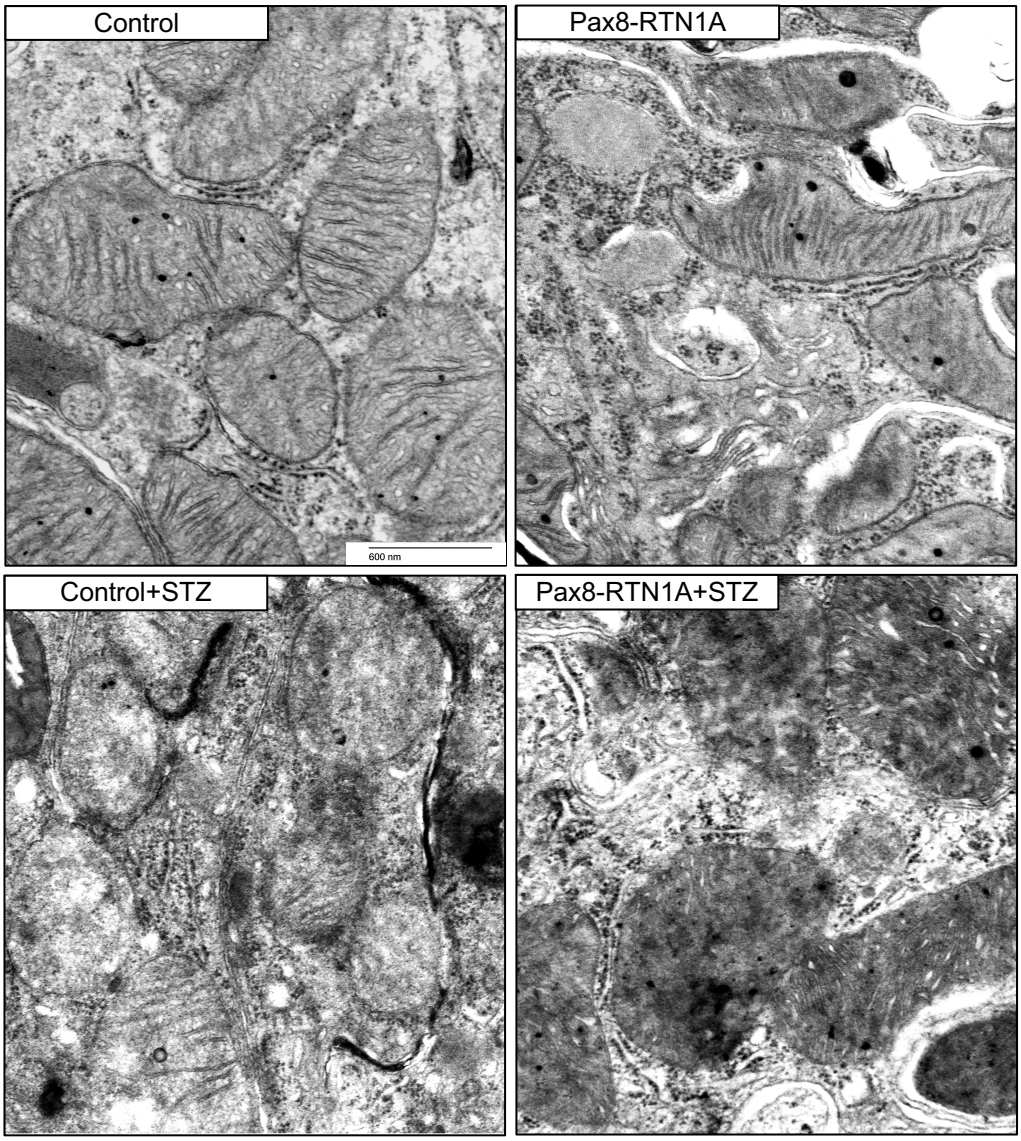

Supp. Fig. 4: Ultrastructural analysis of ER-mitochondria contacts in control and diabetic kidneys. Representative transmission EM images of mitochondria connected to the ER in kidney from WT, RTN1A^{OVE} , WT+STZ, RTN1A^{OVE} +STZ mice and examples of distances measured are denoted.

S. Figure 5

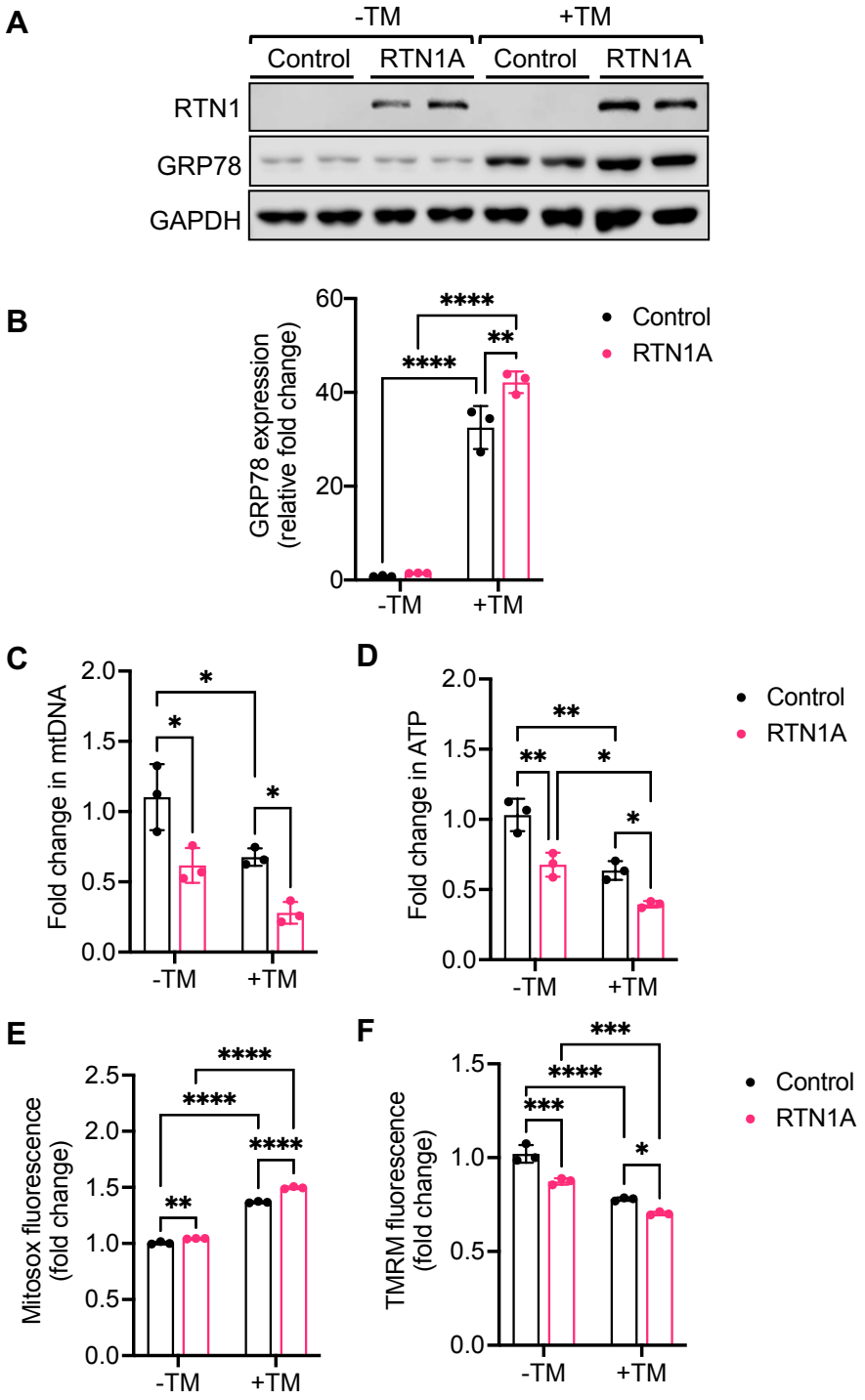

Supp. Figure 5: RTN1A exacerbates tunicamycin-induced ER-stress and mitochondrial dysfunction in HK2 cells. Control or RTN1A overexpressing HK2 cells were treated with or without tunicamycin (TM, 25ng/ml for 24 hours). (A) Western blot analysis of RTN1A and GRP78 expression in cells with or without TM treatment. (B) Real-time PCR analysis of *GRP78* expression. (C) Average fold change in mtDNA content. (D) Average fold change in ATP levels. (E) Average fold change in MitoSOX signals. (F) Average fold change in TMRM signals. (n=3 samples per group,).*p<0.05, **p<0.01, ***p<0.001 and ****p<0.0001 between indicated groups by two-way ANOVA with Tukey's post hoc analysis.

S. Figure 6

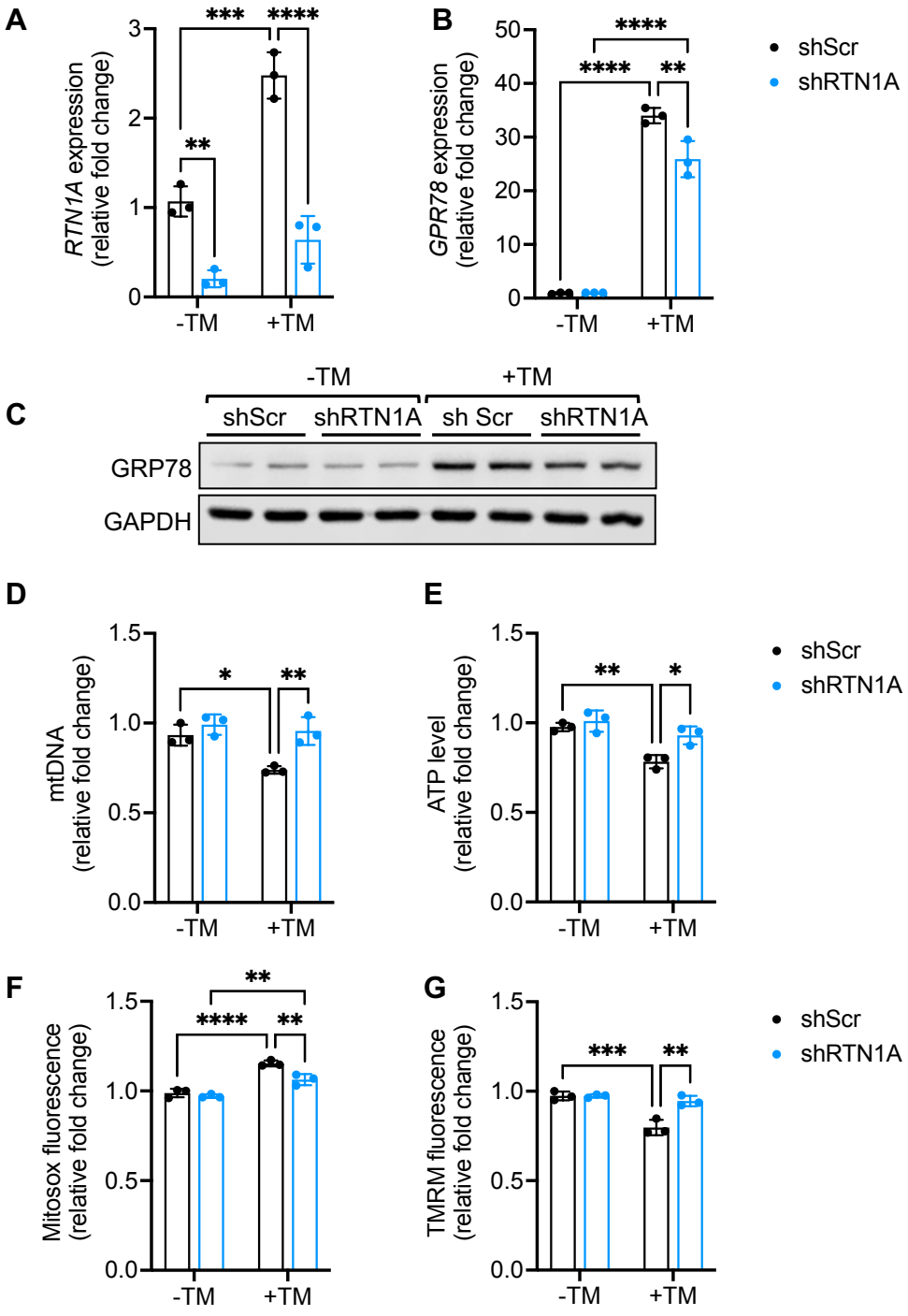

Supp. Figure 6: RTN1A knockdown attenuates tunicamycin-induced ER-stress and mitochondrial dysfunction in HK2 cells. Control HK2 (scrambled shRNA, shScr) or HK2 with RTN1A knockdown (shRTN1A) were treated with or without tunicamycin (TM, 25ng/ml for 24 hours). (A-B) Real-time PCR analysis of *RTN1A* (A) and *GRP78* (B) expression. (C) Western blot analysis of GRP78 expression. (D) Average fold change in mtDNA content. (E) Average fold change in ATP levels. (F) Average fold change in MitoSOX signals. (G) Average fold change in TMRM signals. (n=3 samples per group,).*p<0.05, **p<0.01, ***p<0.001 and ****p<0.0001 between indicated groups by two-way ANOVA with Tukey's post hoc analysis.

S. Figure 7

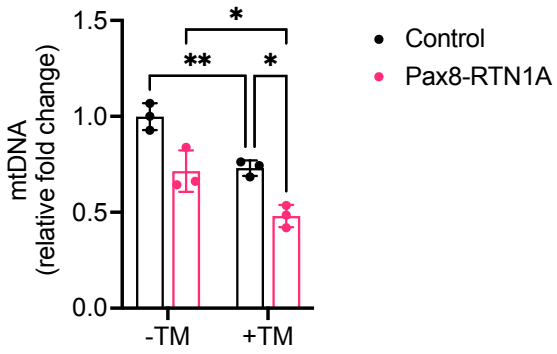

Supp. Figure 7: RTN1A exacerbates tunicamycin-induced ER-stress and mitochondrial dysfunction in primary TECs. Control or RTN1A overexpressing primary tubular cells were treated with or without tunicamycin (TM, 25ng/ml for 24 hours). Average fold change in mtDNA content is shown (n=3 samples per group). *p<0.05 and **p<0.01 between indicated groups by two-way ANOVA with Tukey's post hoc analysis.

S. Figure 8

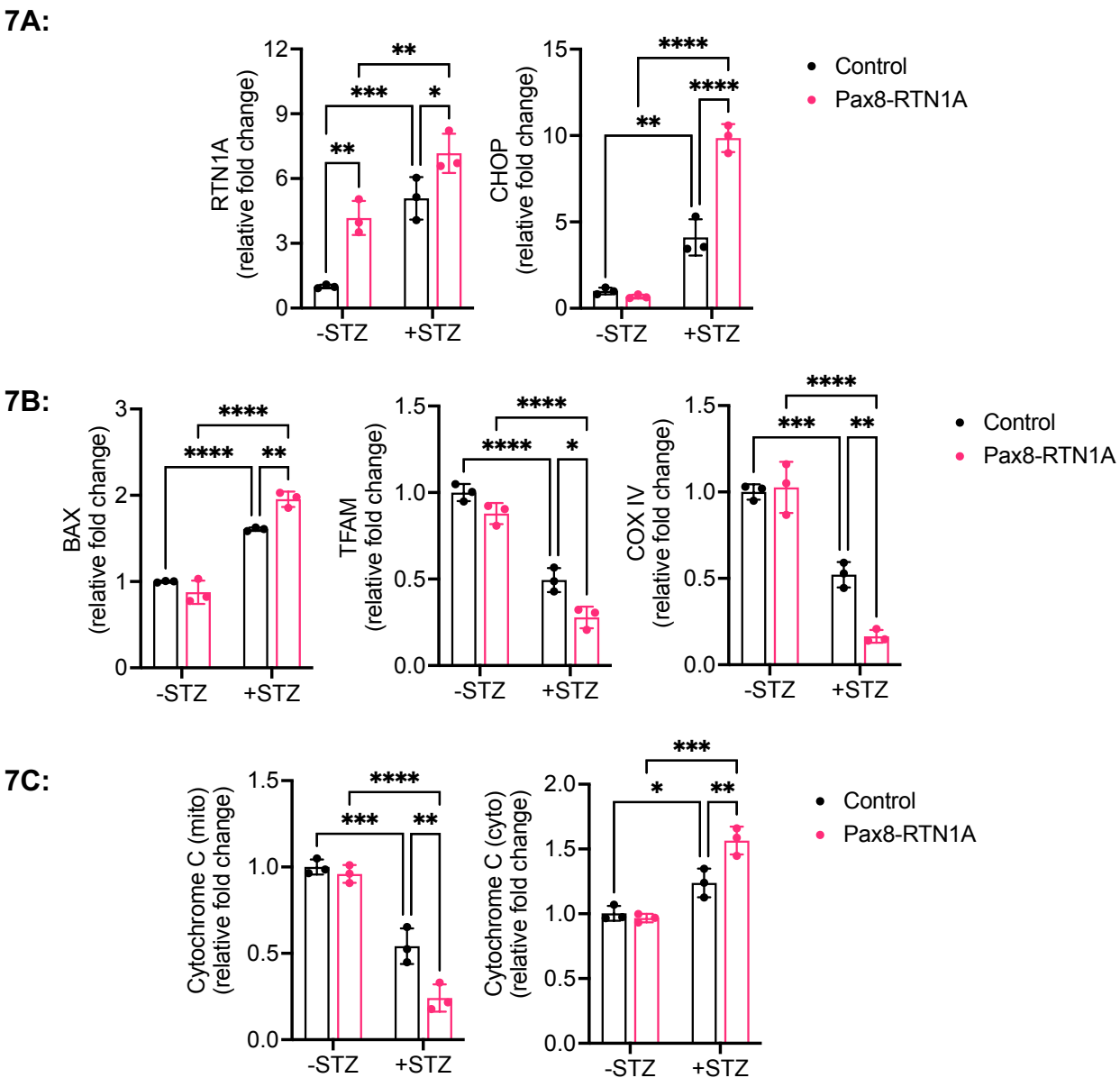

Supp. Figure 8: Densitometric analysis of western blots in Figure 7. (A) Western blot analysis of RTN1A and CHOP in kidneys of control and diabetic mice. (B) Western blot analysis of BAX, TFAM, and COX IV in kidneys of control and diabetic mice. (C) Western blot analysis of cytochrome C in the mitochondrial and cytoplasmic fractions of kidney cortices. *p<0.05, **p<0.01, ***p<0.001 and ****p<0.0001 between indicated groups by two-way ANOVA with Tukey's post hoc analysis.

S. Figure 9

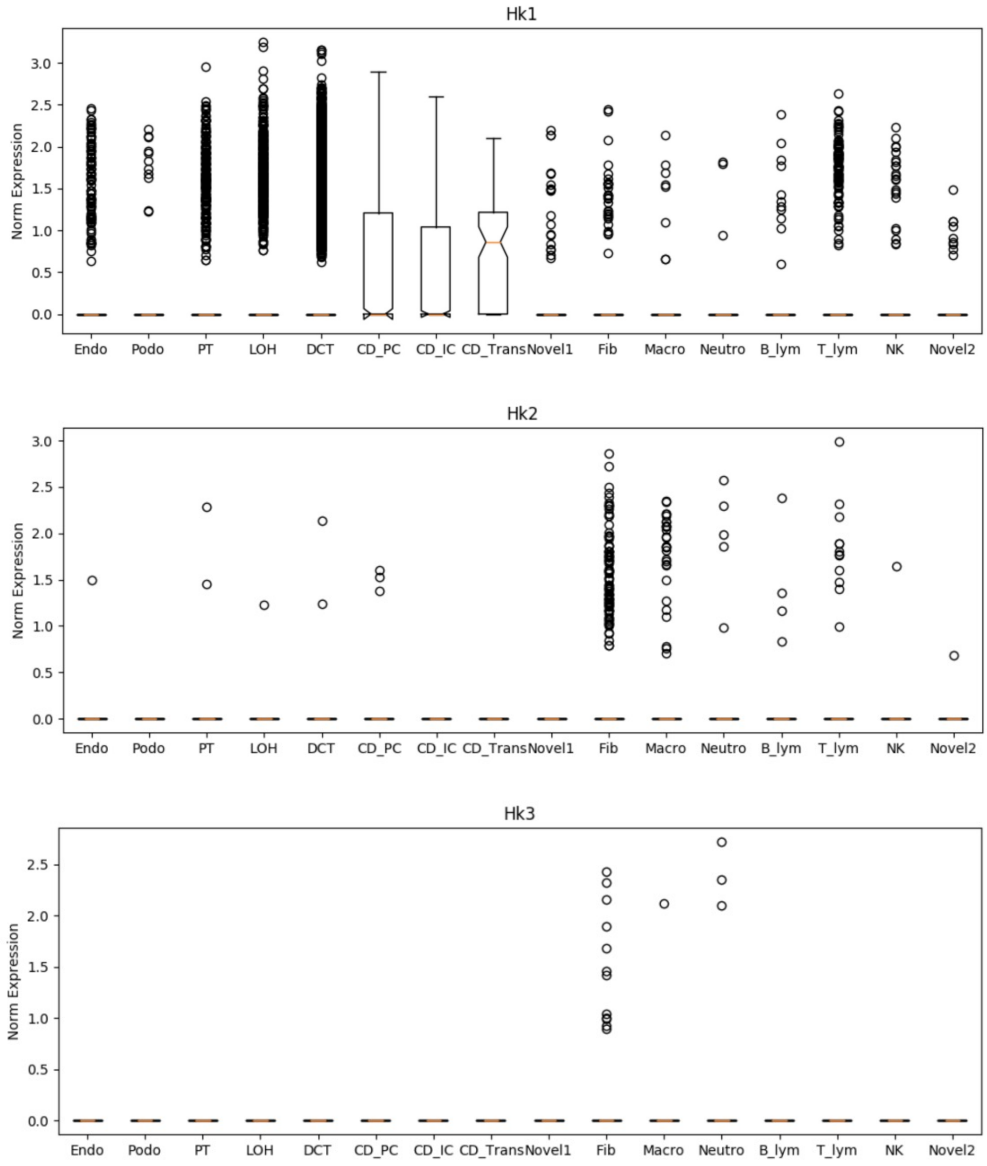

Supp. Figure 9: Kidney cell-specific expression of Hexokinases in mouse kidneys. The expression of *Hk1*, *Hk2*, and *Hk3* in mouse kidney single-cell transcriptome from Park et al. 2018. *Hk1* is abundantly expressed in all tubular cell types in mouse kidneys.

S. Figure 10

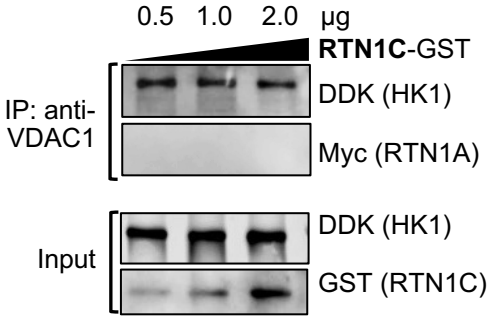

Supp. Figure 10: RTN1C does not interfere with HK1-VDAC1 interaction. Immunoprecipitation was performed using purified recombinant proteins (DDK-tagged HK1, His-tagged VDAC1, and GST-tagged RTN1C). Interaction of HK1 and VDAC1 was assessed with increasing amounts of RTN1C using anti-His antibody and immunoblotted with DDK and Myc antibodies.

S. Figure 11

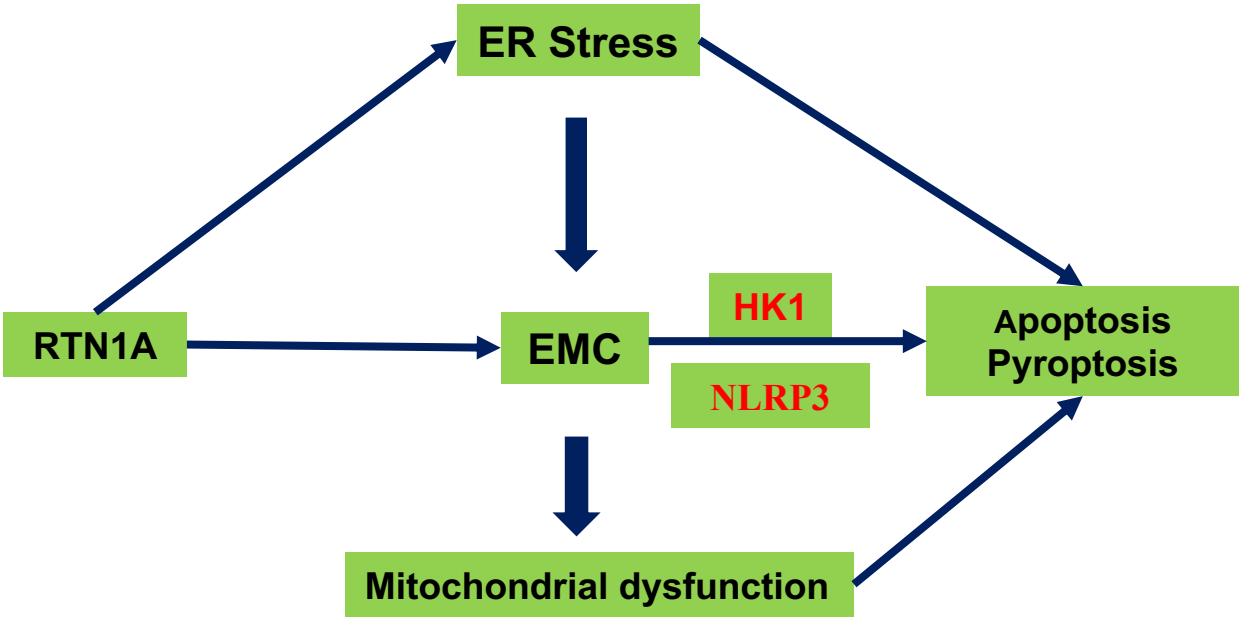

Supp. Figure 11: Summary of the mechanisms by which RTN1A injury kidney cells to promote kidney disease progression

Table S1. List of top 20 RTN1A-interacting proteins. Top 20 RTN1A-interacting proteins are shown in the highest ratio of spectra counts between RTN1A-expressing and control (Ctrl) HEK293 cells. Gene names encoding the proteins are indicated in parenthesis.

Top 20 RTN1A-interacting proteins	Accession Number	Molecular Weight	Spectra counts (Ctrl)	Spectra counts (RTN1A)	Ratio (RTN/Ctrl)
Tubulin beta-2A chain (TUBB2A)	Q13885	50 kDa	0	160	81.0
Tubulin beta-6 chain (TUBB6)	Q9BUF5	50 kDa	0	87	44.5
Heterogeneous nuclear ribonucleoprotein L (HNRNPL)	P14866	64 kDa	0	27	14.5
Hexokinase-1 (HK1)	P19367	102 kDa	0	25	13.5
Tubulin alpha chain-like 3 (TUBAL3)	A6NHL2	50 kDa	0	21	11.5
Keratin, type I cuticular Ha4 (KRT34)	O76011	49 kDa	0	19	10.5
Staphylococcal nuclease domain-containing protein 1 (SND1)	Q7KZF4	102 kDa	0	17	9.5
Septin-7 (SEPT7)	Q16181	51 kDa	0	17	9.5
Serine/arginine repetitive matrix protein 2 (SRRM2)	Q9UQ35	300 kDa	0	16	9.0
Heterogeneous nuclear ribonucleoprotein H2 (HNRNPH2)	P55795	49 kDa	0	16	9.0
ATP synthase subunit beta, mitochondrial (ATP5B)	P06576	57 kDa	3	43	9.0
X-ray repair cross-complementing protein 5 (XRCC5)	P13010	83 kDa	1	25	9.0
Dolichyl-diphosphooligosaccharide--protein glycosyltransferase subunit 1 (RPN1)	P04843	69 kDa	1	22	8.0
Septin-11 OS=Homo sapiens (SEPT11)	Q9NVA2	49 kDa	1	21	7.7
ADP/ATP translocase 3 (SLC25A6)	P12236	33 kDa	0	13	7.5
ATP-citrate synthase (ACLY)	P53396	121 kDa	0	12	7.0
Septin-6 (SEPT6)	Q14141	50 kDa	0	12	7.0
NADH-ubiquinone oxidoreductase 75 kDa subunit, mitochondrial (NDUFS1)	P28331	79 kDa	0	12	7.0
Superkiller viralicidic activity 2-like 2 (SKIV2L2)	P42285	118 kDa	0	11	6.5
BAG family molecular chaperone regulator 2 (BAG2)	O95816	24 kDa	0	11	6.5

Supplemental Methods

Measurement of Urine Albumin and Creatinine

Blood urea was measured using a commercially available kit (BioAssay Systems, #DIUR-100) according to the manufacturer's instructions. Urine albumin was quantified by a commercially available ELISA kit (Bethyl Laboratories, #E99-134). Urine creatinine levels were measured in the same samples using the creatinine assay kit (BioAssay Systems, DICT-500). The urine albumin excretion rate was expressed as the ratio of albumin to creatinine for spot urine. 24-hour urine collections in the metabolic cages were also used for the determination of total urinary albumin excretion.

Kidney histology and tubular injury scoring

Kidneys were removed and fixed with 4% paraformaldehyde 16 hours at 4 °C. The 4μm sections were cut from paraffin-embedded kidney tissues. Sections were stained with periodic acid–Schiff (PAS) for histology analysis. Assessment of the mesangial and glomerular cross-sectional areas was performed by pixel counts on a minimum of 20 glomeruli per section in a blinded fashion, under 400x magnification (Zeiss AX10 microscope, Carl Zeiss). Tubular injury was scored in the cortical region on a scale from 0-4, based on tubular dilatation, loss of brush border and tubular structure, and tubular atrophy: 0 (normal); 1 (less than 25%); 2 (25%-50%); 3 (50%-75%); and 4 (more than 75%). Scoring was performed on minimum of 30 cortical fields (200x original magnification) per PAS-stained kidney section per mouse and averaged (n=5 mice per group). Nonparametric Mann-Whitney test was applied for statistical analysis of tubular injury scores.

Picrosirius Red and Masson Trichrome Staining

Picrosirius red staining and Masson Trichrome Staining were used to evaluate renal fibrosis according to the manufacturer's instructions (Abcam, #ab150681 and Thermo Fisher Scientific, #87019). The staining intensities were quantified by Image J.

Transmission Electron Microscopy (TEM)

Tissues were fixed in 2.5% glutaraldehyde with 0.1M sodium cacodylate (pH 7.4) for 72 hr at 4°C. Samples were further incubated with 2% osmium tetroxide and 0.1M sodium cacodylate (pH 7.4) for 1 hr at room temperature. Ultrathin sections were stained with lead citrate and uranyl acetate and viewed on a Hitachi H7650 microscope. Briefly, negatives were digitized, and images with a final magnitude of up to X7,000 were obtained. The morphology of mitochondria was examined in the kidney of the mice. Quantification of dysmorphic mitochondria was performed as previously described [1, 2]. Briefly, an average of 50 mitochondria were analyzed per mouse kidney (n=3 mice per group), and dysmorphic mitochondria were defined as mitochondria with a focal loss of visible cristae, clustering of residual cristae at the peripheral mitochondrial membrane, and fragmented (<2μm in length). The distance of EMCs on TEM images were quantified as previously described [3]. Briefly, the ER-outer mitochondrial membrane (OMM) distance was measured in 10-50 measurements per field. ER-OMM apposition was measured considering the following three subsets of ER-OMM distances: closely associated < 5 nm, between 6 and 10 nm, and between 11 and 20 nm. Per each subset quantitation of the ER length adjacent to mitochondria was calculated and normalized by mitochondrial perimeter.

Antibodies for immunostaining and western blot analyses

Following antibodies were used: anti-RTN1A (MON162, Abcam #ab8957), anti-CHOP (Cell Signaling Technology, #2895), anti-BAX (Cell Signaling Technology, #2772), anti-TFAM (Abcam, #ab131607), anti-COX IV (Cell Signaling Technology, #4850), anti-Cytochrome C (Cell Signaling Technology, #4272), anti-HK1 (Cell Signaling Technology, #2024), anti-KIM1 (R&D, AF1817), anti-phospho-PERK (Santa Cruz Biotechnology, sc-32577), and anti-GAPDH (Cell Signaling Technology, #2118).

Immunohistochemistry

Immunohistochemistry staining was performed on formalin-fixed, paraffin-embedded kidney sections. Sections were deparaffinized and heated in citrate for antigen retrieval. Then, sections were added with H_2O_2 to ablate endogenous peroxidase and blocked with diluted horse serum for 1 hour at room temperature, followed by incubation with primary antibody overnight at 4°C. The next day, sections were washed three times with phosphate-buffered saline and then incubated with secondary antibody for 30 min. Archival human biopsy specimens of healthy donor nephrectomies and DN were collected at Icahn School of Medicine at Mount Sinai under a protocol approved by the Institutional Review Board.

Immunofluorescence

Co-immunostaining of RTN1A was performed on frozen mouse kidney tissues using anti-RTN1A (MON162). Fluorescein-conjugated lectins (*Lotus tetragonolobus* agglutinin and *Dolichos biflorus* agglutinin, Vector Laboratories, cat# FL-1321-2 and FL1301) were incubated with secondary antibody to visualize the proximal and distal collecting duct cells. After washing, sections were incubated with a fluorophore-linked secondary antibody and mounted with aqueous mounting with DAPI. For quantification of immunostaining, 10-20 non-overlapping fields were randomly selected per mouse kidneys and quantified using ImageJ software (National Institutes of Health).

TUNEL assay

TUNEL staining was performed according to the manufacturer's instructions (Promega, #PRG3250). TUNEL-positive cells of per kidney field (10-15 fields per kidney) were counted in each sample.

Cell culture

HK2 and HEK293T cells were obtained from ATCC (#CRL-2190 and CRL-3216) and cultured according to their instructions. Human primary renal proximal tubular cells were obtained from Lonza (# CC-2553) and cultured as instructed. Cells were stimulated with Tunicamycin (Sigma-Aldrich) or high glucose as described in the legends. Cells were cultured at 37°C (5% CO_2, 90% humidity). For transient transfections, Viafect transfection Reagent kit (Promega) was used to transfect HK2 cells and PolyJet reagent for HEK293T cells (SignaGen Laboratories). Overexpression vectors of RTN1A were obtained from Thermo Scientific and different clones of shRNA for RTN1 were obtained from Open Biosystems. The efficiency of overexpression and knockdown was confirmed by both western blot and real-time PCR. The expression constructs for WT-RTN1A-FLAG and RTN1C-FLAG were generated using a PCR-based mutagenesis method. To generate the human RTN1A-FLAG WT construct, we used the following primers: 5'-TGC TAG CCA CCA TGG CCG CGC CGG GGG ATC CAC AGC GAG CTC ATC ATC G-3' and 5'-AGG TCG ACA TCG ATT ATT TGT CAT CGT CGT CCT TGT AGT CCA TGA TAT CCT CAG CGT GCC TCT TAG C-3'. For cloning human RTN1C-FLAG, the primers used were 5'-TAG CTA GCC ACC ATG CAG GCC ACT GCC GAT TCC ACC AAG ATG GAC TGT GTG TGG AGC AAC TGG AAA AGT CAG GCT ATT GAC CTG TTG TAT TGG-3'.

Lentiviral preparation and infection

HEK293T cells were transfected with either lentiviral plasmid expressing RTN1 shRNA sequence pGIPZ-shRTN1 (Open biosystems) or control scrambled sequence, pGIPZ-scramble, plus psPAX2 packaging plasmid and pMD2.G envelop plasmid using PolyJet transfection reagent according to the manufacturer's protocol (SignaGen Laboratories). Forty-eight hours after transfection, the lentiviral particles were harvested from HEK293T cell culture medium. Concentrated lentiviral particles were used to infect HK2 cells.

Western Blot Analysis

Cells or tissues were lysed with buffer containing 1% NP40 with a protease and phosphatase inhibitor cocktail. Western blots were developed with the enhanced chemiluminescence system and imaged with Odyssey Fc Imaging System (LI-COR Biosciences).

Real-Time PCR
Primers for real-time PCR were designed by using the National Center for Biotechnology Information Primer BLAST tool. PCR was performed using SYBR Green Master Mix (Applied Biosystems) and the Applied Biosystems 7500 Real-Time PCR system. Gene expression was normalized to housekeeping gene GAPDH and fold change in expression relative to the control group was calculated using the $2^{-\Delta\Delta Ct}$ method.

Isolation of Mitochondria
Mitochondria from kidney cortex were isolated using a Mitochondria Isolation Kit for Tissue (Thermo Fisher Scientific, #89874) according to the manufacturer's protocol. Isolated mitochondria protein concentration was determined by the Bradford method.

mtDNA Copy Number
Total DNA was extracted from the kidney cortex or cells by using a DNeasy Tissue Kit (69506; QIAGEN Sciences, Germantown, MD) following the manufacturer's instructions. The primer oligonucleotides listed in Table 2 were designed by using the National Center for Biotechnology Information Primer BLAST tool. Real-time PCR was performed for the detection of mtDNA copy numbers. Relative mtDNA copy numbers were normalized to the nuclear 18S rRNA gene and calculated using the $2^{-\Delta\Delta Ct}$ method.

ATP level
ATP levels were determined by using a bioluminescence assay kit (Thermo Fisher Scientific, #A22066) according to the manufacturer's instructions.

Mitochondrial ROS
Mitochondrial ROS production in HK2 cells was measured using mitoSOX (Invitrogen, #M36008). Briefly, the adherent HK2 cells were washed twice with PBS and incubated in the dark with mitoSOX (5uM; 10 minutes at 37°C). cells were washed with PBS. For quantitation of mitochondrial ROS production, the ROS levels were analyzed by flow cytometry.

Mitochondrial membrane potential
The Mitochondrial membrane potential of HK2 cells was monitored by using TMRM, MMP-sensitive, fluorescent dye (Thermo Fisher Scientific, #T668 or M20036). Briefly, the adherent HK2 cells were washed twice with PBS and incubated in the dark with TMRM (100nM; 30 minutes at 37°C). Cells were washed with PBS. Fluorescence quantitation was detected with flow cytometry.

Immunoprecipitation
For immunoprecipitation of cell lysates, lysates of cells expressing FLAG-tagged WT-RTN1A, control vector, RTN1C incubated with anti-FLAG antibody overnight at 4°C, and the immunoprecipitated proteins were immunoblotted using anti-RTN1A, anti-RTN1C, anti-HK1 and anti-VDAC antibodies as indicated. For immunoprecipitation using purified recombinant human proteins, 1µg of recombinant His-tagged VDAC1 (Creative Biomart, #VDAC1-19H) was first immobilized on beads (ThermoFisher #10103D) and incubated with 1µg of purified recombinant HK1 (LSBio, #LS-G65898) and varying amounts either recombinant RTN1A (Antibodies-online, #ABIN2730745) or RTN1C (Novus Biologicals, H00006252) under rotation for 2h at 4°C. After washing, proteins were eluted in sample buffer and analyzed by Western blot analysis.

Proximity ligation assay: PLA were performed using a Duolink assay with brightfield detection (Millipore Sigma, #Duo92101) according to the manufacturer's instructions. Briefly, HK2 cells with or without RTN1A overexpression were cultured on collagen-coated coverslips under normal or high glucose conditions. Cells were then fixed, permeabilized, and incubated with primary antibody pairs, IP3R-3 and anti-VDAC1 overnight at 4°C. After washing, cells were incubated with secondary PLA probes (anti-Rabbit PLA probe Plus and anti-

Mouse PLA probe Minus) for 1 h at 37°C. After washing, cells were incubated with Duolink ligation mix for 30 min at 37°C, followed by amplification for 100 minutes at 37°C. Nuclei were stained with DAPI, mounted, and imaged under the fluorescence microscope. Quantification of the PLA red fluorescent dots was performed using ImageJ, on 10 sets of images acquired with the same optical settings per conditions.

Supplemental References

1. Herlitz LC, Mohan S, Stokes MB*, et al.* Tenofovir nephrotoxicity: acute tubular necrosis with distinctive clinical, pathological, and mitochondrial abnormalities. *Kidney Int* 2010; **78:** 1171-1177.
2. Brooks C, Wei Q, Cho SG*, et al.* Regulation of mitochondrial dynamics in acute kidney injury in cell culture and rodent models. *J Clin Invest* 2009; **119:** 1275-1285.
3. D'Eletto M, Rossin F, Occhigrossi L*, et al.* Transglutaminase Type 2 Regulates ER-Mitochondria Contact Sites by Interacting with GRP75. *Cell Rep* 2018; **25:** 3573-3581 e3574.
4. Potapova TA, Sivakumar S, Flynn JN*, et al.* Mitotic progression becomes irreversible in prometaphase and collapses when Wee1 and Cdc25 are inhibited. *Mol Biol Cell* 2011; **22:** 1191-1206.